






Research article

Mechanical, thermal and optical properties of natural rubber films with different types of bifunctional aldehydes as curing agents

Rawiporn Promsung¹, Yeampon Nakaramontri², Claudia Kummerlöwe³, Jobish Johns⁴, Norbert Vennemann³, Ekwipoo Kalkornsurapraee^{1*}

¹Division of Physical Sciences, Faculty of Science, Prince of Songkla University, Hat-Yai, Thailand

²Sustainable Polymer & Innovative Composite Materials Research Group, Department of Chemistry, Faculty of Science, King Mongkut's University of Technology Thonburi, Bangkok, Thailand

³Faculty of Engineering and Computer Science, University of Applied Sciences Osnabrück, Osnabrück, Germany

⁴Department of Physics, Rajarajeswari College of Engineering, Bangalore, India

Received 5 February 2022; accepted in revised form 7 April 2022

Abstract. A new simple system to vulcanize natural rubber (NR) latex at low temperature (50 °C) using different bifunctional aldehydes has been proposed. Bifunctional aldehydes with different number of carbon atoms present in the chemical structure, including glyoxal (GX) with 2 carbon atoms, glutaraldehyde (GA) with 5 carbon atoms and phthaldialdehyde (PA) with 8 carbon atoms were added into natural rubber latex. The mechanical, thermal and optical properties of the crosslinked NR were studied. The formation of crosslinking in the cured NRs was confirmed using infrared spectroscopy (ATR-FTIR). A new absorption peak was found at 1589 cm⁻¹ for –NH bending of secondary amine in the case of cured NRs when compared to uncured NR. Universal testing machine (UTM), dynamic mechanical thermal analysis (DMA), thermogravimetric analyzer (TGA) and temperature scanning stress relaxation (TSSR) were employed to study the tensile and thermal properties of cured NRs. Results revealed that the GA cured NR exhibited superior mechanical properties in terms of 100% modulus, tensile strength and hardness up to 2.13, 6.38 MPa and 54.67 Shore A, respectively. Furthermore, GA cured NR showed the highest crosslink density (72.40 mol/m³) and also showed better thermal properties among the different curing systems. The optical properties in terms of transparency of cured NRs were studied. It was noticed that PA cured NR gave more transparency and hence it can be introduced in developing materials for sensor applications.

Keywords: rubber, mechanical properties, thermal properties, bifunctional aldehydes, transparency

1. Introduction

Natural rubber (NR) is a renewable resource collected from the tree *Hevea brasiliensis* with the chemical structure of *cis*-1,4- polyisoprene [1, 2]. NR is an important elastomeric material used to produce rubber articles such as tires, automotive parts, gloves, condoms, medical devices, and so on [2, 3]. Various outstanding properties of NR including elasticity, strength, elongation at break, and resilience make the

material suitable for many flexible engineering applications. However, NR consists of a small amount of non-rubber components such as proteins, lipids, carotenoids *etc.* [4, 5]. Polyphenol is the most important component that causes discoloration of NR [6, 7]. It is due to the presence of polyphenols that *ortho*-quinones are generated by oxidation. These quinones react with the non-rubber constituents such as protein present in the NR latex that, changes the color

*Corresponding author, e-mail: ekwipoo.k@psu.ac.th

© BME-PT

of NR products into yellowish [6, 7]. Therefore, the discoloration of NR is a major disadvantage of NR products and it should be minimized.

The vulcanization process is one of the very important processes for rubber to enhance its stability and properties. There are many vulcanization techniques widely used such as sulfur, peroxide and phenolic resin curing. However, these curing systems need high temperatures with various chemicals [8]. Recently, a system for curing rubber including a bifunctional aldehyde reagent was reported [9]. A bifunctional aldehyde reagent is a crosslinking agent that consists of long carbon main chains connecting the two reactive end-groups [10]. These aldehyde end-groups could be crosslinked to the NR molecules [10]. Furthermore, this aldehyde reagent has the ability to vulcanize NR molecules easily at low temperature and it is a cost-effective vulcanization method [8]. Currently, vulcanization of NR latex using a bifunctional aldehyde reagent has been proposed by various researchers [8, 9, 11–13]. In 2012, Johns *et al.* [9] have initially reported the low-temperature vulcanization of NR using glutaraldehyde (GA) as a curing agent. It was observed that NR can be vulcanized using GA at 50 °C without any specific activators and accelerators. Vulcanization of this system can be divided into two steps. Firstly, GA reacts with ammonia present in NR latex to generate pentane-1,5-diylidenediamine. Secondly, NR molecular chains were crosslinked *via* ‘ene’ reaction by pentane-1,5-diylidenediamine. Crosslinking of NR molecules in the presence of GA ammonia was confirmed by FT-IR spectra. In addition, Promsung *et al.* [12] reported that the curing agent (GA) has not only reacted with the ammonia present in NR latex but also reacted with the amino groups of protein molecules. Therefore, the interaction between GA and protein might prevent the discoloration of NR latex by inhibiting the reaction between quinones and protein [12]. However, there are no reports available on the low-temperature vulcanization of NR latex using other bifunctional aldehydes as curing agents.

The present work is aimed to prepare NR vulcanizates using three bifunctional aldehydes with different number of carbon atoms in the chemical structure as curing agents including glyoxal (GX) with 2 carbon atoms, glutaraldehyde (GA) with 5 carbon atoms and phthaldialdehyde (PA) with 8 carbon atoms. Curing of NR with three types of bifunctional aldehyde was confirmed from the ATR-FTIR spectra

and the crosslinking density was determined by using the temperature scanning stress relaxation (TSSR) technique. Mechanical, thermal and optical properties of the resulting NR vulcanizates were also investigated from the tensile test, dynamic mechanical thermal analysis (DMTA), thermogravimetric analyzer (TGA), TSSR and color spectrophotometer.

2. Experimental

2.1. Materials

Natural rubber (NR) in the form of commercial high ammonia latex (HA latex) with 60% dry rubber content (DRC) was purchased from Chalong Latex Industry (Songkhla, Thailand). Glyoxal (GX) was supplied by Boss Optical Limited Partnership, Songkhla, Thailand. Glutaraldehyde (GA) curing agent was purchased from Wing Great Industry Co., Ltd, (Bangkok, Thailand). Phthaldialdehyde (PA) reagent was purchased from Sigma-Aldrich (Missouri, USA).

2.2. Preparation of latex vulcanizates using bifunctional aldehydes

12.5 % solutions of GX, GA and PA were prepared by diluting in distilled water. The solution was slowly added to the latex, where the ammonia content was already adjusted according to ASTM D-1076-02. The mixture was continuously stirred for approximately 1 min at room temperature. A molar ratio of 2:1 (ammonia:aldehyde) was maintained during the entire course of the investigation. The latex compound was then transferred into a glass plate of 130×130×2 mm³ and dried in a hot air oven at 50 °C for at least 24 hours to attain a constant weight [12, 13]. The latex vulcanizates were finally removed and kept in a desiccator for another 24 h before performing the characterizations.

3. Characterization

3.1. Attenuated total reflectance-Fourier transform infrared (ATR-FTIR) analysis

The ATR-FTIR spectra were used to clarify the crosslinking of NR molecular chains using a Bruker FTIR spectrometer (Model Vertex 70, Ettlingen, Germany). The spectra were recorded on transmittance mode in the range of 4000–400 cm⁻¹ with 32 scans at a resolution of 4 cm⁻¹.

3.2. Mechanical testing

Tensile testing of the vulcanizates was performed according to the ASTM D412 using a universal testing

machine (Model H10KS, Hounsfield, England). The samples were cut into dumbbell-shaped specimens and the test was carried out with a crosshead speed of 500 mm/min at room temperature. Tensile properties in terms of modulus, tensile strength and elongation at break were obtained from the stress-strain plot. In case of the hardness of the samples, the tests were performed using a Shore A durometer (Frank GmbH, Hamburg, Germany) according to the ASTM D2240.

3.3. Dynamic mechanical thermal analysis (DMTA)

Dynamic mechanical thermal analysis (DMTA) was performed using dynamic mechanical analyzer DMA 1 (Mettler Toledo, Greifensee, Switzerland). The experiment was conducted in a dual cantilever bending mode at a frequency of 1 Hz and strain magnitude of 0.1% with a heating rate of 5 K/min over the range of temperature of -100 to 80 °C/min.

3.4. Thermal testing

A thermogravimetric analyzer (TGA) (Mettler Toledo AG, Greifensee, Switzerland) was adopted to evaluate the thermal stability of cured-NR vulcanizates. To perform the measurement, 10 mg of the sample was taken in the crucible and kept in the TGA chamber. The test was conducted in the temperature range of 40 – 600 °C at a heating rate of 10 °C/min under a nitrogen atmosphere. During the test, the sample was held at 600 °C for 10 min and the atmosphere was switched to the oxygen atmosphere before continuing the test to 800 °C at the same heating rate.

3.5. Thermo-mechanical testing

Thermo-mechanical properties and estimated crosslink density of the cured-NR samples were analyzed using an advanced technique, namely temperature scanning stress relaxation (TSSR) (Brabender GmbH Duisburg, Germany). The vulcanizates were prepared as dumbbell-shaped specimens following the ISO527 type 5A. Then, the specimen was placed in the electrically heated test chamber and pre-conditioned at 100% strain at room temperature for 2 h. Further, the non-isothermal test was performed by raising the temperature with a constant rate of 2 °C/min until the sample gets ruptured. The initial forces from TSSR results were obtained from the force at the beginning of the non-isothermal test. Then, the normalized

force curve was plotted as a function of temperature. It is noted that the T_x indicates the temperature at which force has been reduced by about $x\%$ from the initial force. T_{10} , T_{50} and T_{90} are the temperatures at which the force has been decreased about 10, 50 and 90%, respectively. T_{90} describes the thermal resistance of the material [14].

3.6. Color analysis

Color measurement was performed by using a HunterLab UltraScan pro spectrophotometer (HunterLab, Virginia, USA). The color of cured NRs with different bifunctional aldehyde was measured under Reflectance Specular Included (RSIN) mode. The test provides the color parameter, including L^* , a^* and b^* values.

4. Results and discussion

4.1. Crosslinking of NR molecules

Attenuated total reflectance-Fourier transform infrared (ATR-FTIR)

The ATR-FTIR spectra of pure and cured NR are shown in Figure 1. The curing of NR with different bifunctional aldehydes has been confirmed by comparing the spectra of uncured-NR. Also, Table 1 summarizes the characteristic absorption peaks obtained in the spectra. Peaks at 2924 , 1659 , 1446 and 839 cm^{-1} are assigned to C-H stretching vibrations, C=C stretching vibrations, C-H bending vibrations and C-H out of plane bending vibrations of NR, respectively. After vulcanization, a new peak appears at 1589 cm^{-1} , corresponding to N-H bending vibration of secondary amine originated from ene reaction [9, 12]. Moreover, an additional peak

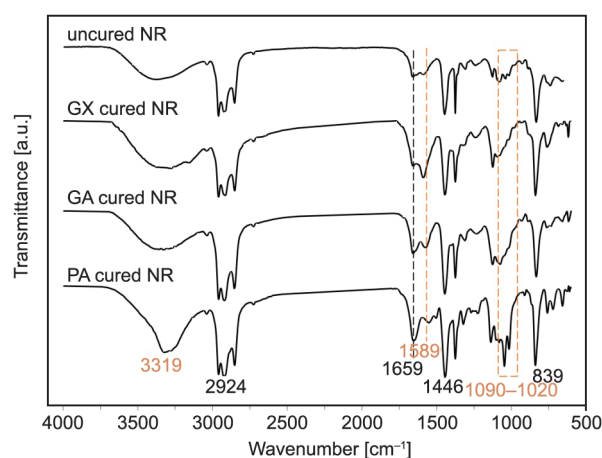


Figure 1. The ATR-FTIR spectra of uncured NR and cured NR with different bifunctional aldehyde curing agents.

Table 1. The absorption peaks of uncured NR and cured NR with different bifunctional aldehyde curing agents.

Wavenumber [cm ⁻¹]	Assignments	NR types with different curing agents.			
		Uncured	GX	GA	PA
839	–C–H out of plane bending vibrations of NR	✓	✓	✓	✓
1090–1020	–C–N stretching vibrations of secondary amine	–	✓	✓	✓
1045	–C–H in-plane bending vibrations of aromatic ring	–	–	–	✓
1446	–C–H bending vibrations of NR	✓	✓	✓	✓
1589	–N–H bending vibrations of secondary amine	–	✓	✓	✓
1615	–C=C stretching vibrations of aromatic ring	–	–	–	✓
1659	–C=C stretching vibrations of NR	✓	✓	✓	✓
2924	–C–H stretching vibrations of NR	✓	✓	✓	✓

appears at 1090–1020 cm⁻¹ due to the –C–N stretching vibrations of secondary amine. It clearly confirms the formation of crosslinks between NR molecules with pentane-1,5-diylidenediamine by ene reaction [9]. In the case of PA cured NR, the absorption peak at 1615 cm⁻¹ of –C=C aromatic secondary stretching is vanished/overlapped with a new peak at 1659 cm⁻¹ corresponds to –C=C stretching vibration of NR. The PA cured NR also shows a peak at 1045 cm⁻¹ corresponding to –C–H in-plane bending vibrations of the aromatic ring [15].

Crosslink density

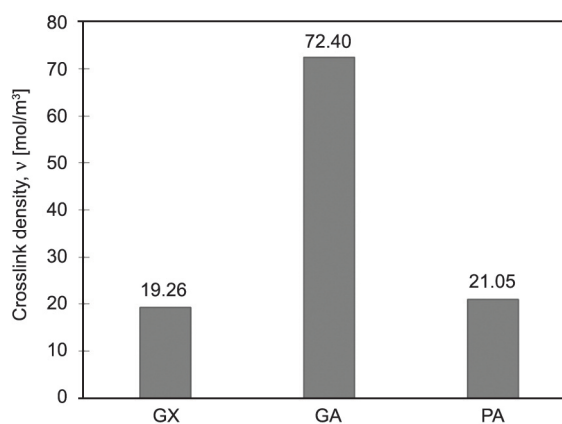
Crosslink density is one of the most important parameters of rubber vulcanizates. Most of the mechanical properties depend on the crosslink density of cured rubber [14]. The crosslink density of cured-NR with different bifunctional aldehydes has been determined by using TSSR measurement. In order to calculate the crosslink density, the initial slope of the normalized force-temperature curve is to be evaluated. According to the theory of rubber elasticity, the temperature coefficient (κ) can be derived from Equation (1) [14]. Also, the crosslink density (ν) of rubber vulcanizates can be determined from Equation (2) [14]:

$$\kappa = \left(\frac{\partial \sigma}{\partial T} \right)_{\lambda, \rho} \quad (1)$$

$$\nu = \frac{\kappa}{R \cdot (\lambda - \lambda^{-2})} \quad \text{with } \nu = \frac{\rho}{M_c} \quad (2)$$

where ρ is the mass density, λ is l/l_0 , l is the final length and l_0 is the initial length of the sample, R is the universal gas constant and M_c is defined as the average molar mass of the elastically active network chains.

Figure 2 shows the crosslink density of NR cured with different bifunctional aldehydes obtained from

**Figure 2.** Crosslink density of cured-NRs obtained from TSSR measurement.

the TSSR measurement. It can be seen that the GA cured-NR exhibited the superior crosslink density among the cured NR samples. This might be due to the presence of five linear carbon atoms in GA molecule, which has a great opportunity to generate crosslinking between molecular rubber chains. On the other hand, GX and PA cured-NRs show lower crosslink density due to the short-chain in its structure that reduces the chance to generate crosslinking between the rubber molecules. Moreover, PA cured-NR with an aromatic ring in its structure might be prevented from generating crosslinking of PA through the rubber chains. The proposed model of vulcanization with different aldehydes is shown in Figure 3.

4.2. Properties of NR vulcanizates

Mechanical properties

The tensile properties of materials can be determined from their respective stress-strain curves. Figure 4 shows the stress-strain curves of cured-NR samples with different bifunctional aldehydes. Also, Table 2 summarizes the overall mechanical properties in terms of modulus, tensile strength, elongation at break

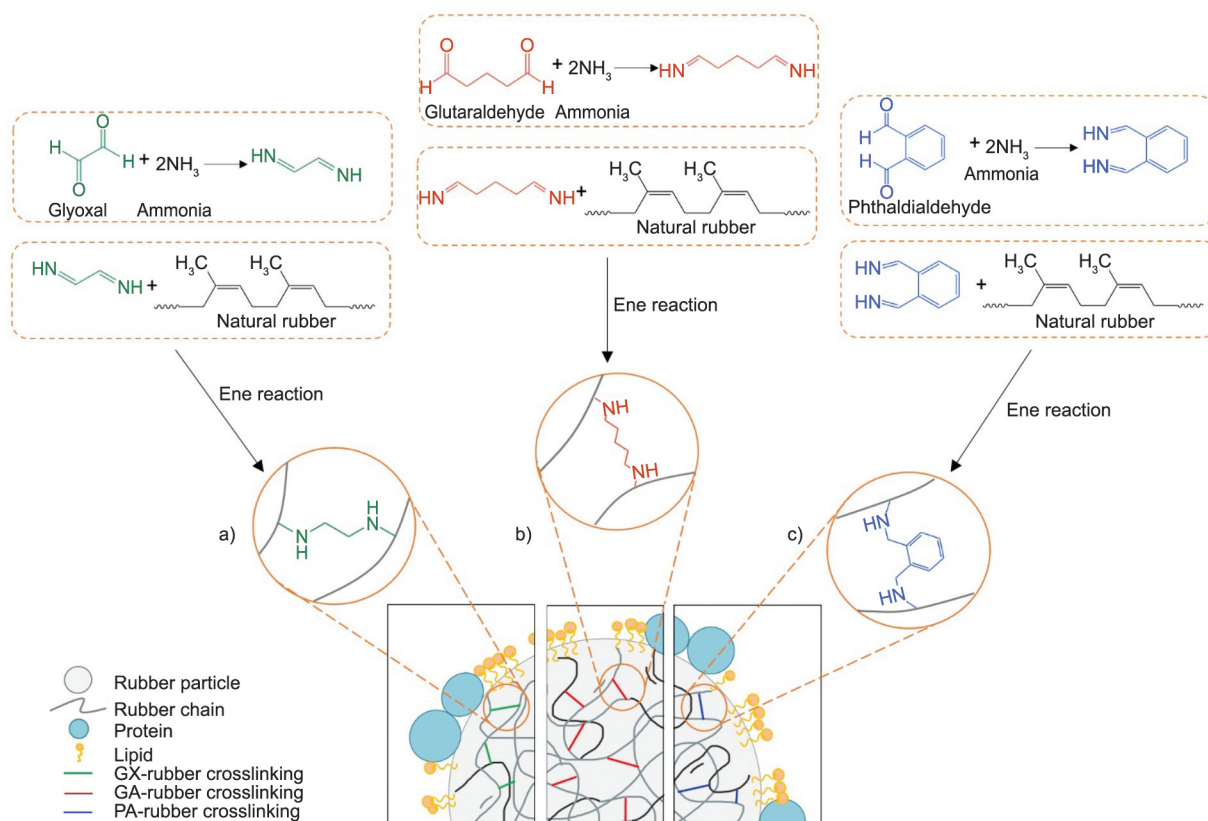


Figure 3. Reaction and the proposed model of crosslinking by bifunctional aldehyde (a) GX (b) GA and (c) PA.

and hardness. The nature of the curve or elastic deformation of GA cured NR is entirely different from

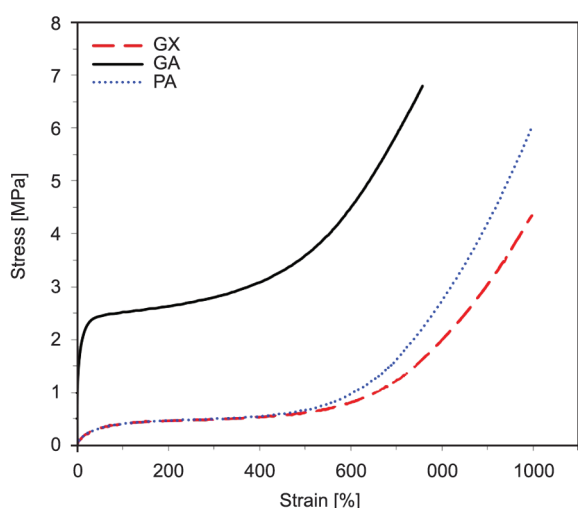


Figure 4. Stress-strain curves of cured NR with different bifunctional aldehydes.

the other two cured NRs. A considerable change in the initial slope can be seen in the stress-strain curves and it indicates the superior elastic modulus and surface hardness of GA cured NR. It is noted that 100% modulus refers to the stiffness of cured NR, while 300 and 500% moduli are mainly referred to as self-reinforcement of the vulcanizates caused by the strain-induced crystallization [16]. It is observed that GA cured NR exhibited the highest moduli compared to the other two cured NRs. This is attributed to the chain entanglement and crosslink density of rubber vulcanizates. Increasing the crosslink density leads to enhancing both the modulus and hardness of the cured-NRs [17]. On the other hand, GX cured-NR and PA cured-NR exhibited lower stress compared to GA-cured NR at the same strain (strain \leq 500%). It also correlates well with the crosslink density results of the cured-NR samples. For the tensile

Table 2. Mechanical properties in terms of modulus, tensile strength and elongation at break of cured NR with different bifunctional aldehydes.

Samples	100% Modulus [MPa]	300% Modulus [MPa]	500% Modulus [MPa]	Tensile strength [MPa]	Elongation at break [%]	Hardness [Shore A]
GX	0.40±0.01	0.48±0.01	0.62±0.02	4.58±0.53	965.1±54.9	24.8±1.0
GA	2.13±0.21	2.55±0.20	3.64±0.30	6.38±0.46	773.6±29.1	54.7±1.5
PA	0.41±0.01	0.50±0.01	0.70±0.10	6.08±0.27	980.0±48.0	27.0±1.0

strength of cured-NR, GX cured-NR shows the lowest value while GA and PA cured-NRs show the same level of tensile strength, about 6 MPa. This is also due to the crosslink density of the vulcanizates, which correlates well with the crosslink density results presented above. Furthermore, PA cured-NR with an aromatic ring in its structure contributed to the higher level of tensile strength [8]. The elongation at break of cured-NR varies in a different manner. GA cured-NR with higher crosslink density shows lower elongation at break than others. This is attributed to the increased number of crosslinks that restricts the movement of NR molecular chains under stress [17].

Thermal analysis

Figure 5 shows the tan delta based on DMTA characterization of cured-NR samples. Also, Table 3 summarizes the glass transition temperature (T_g) of the cured-NR samples. It is observed that GA cured-NR shows the lowest T_g at -62.02 °C, while PA and

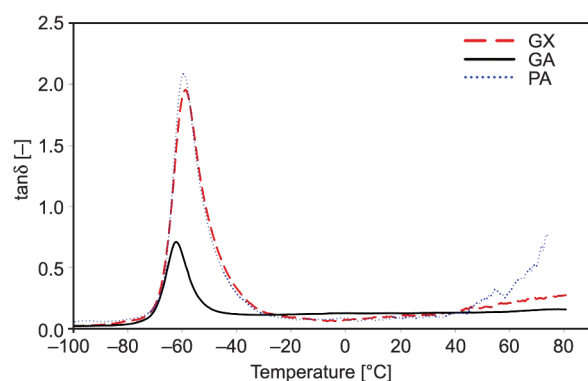


Figure 5. Tan δ of cured NR with different bifunctional aldehydes.

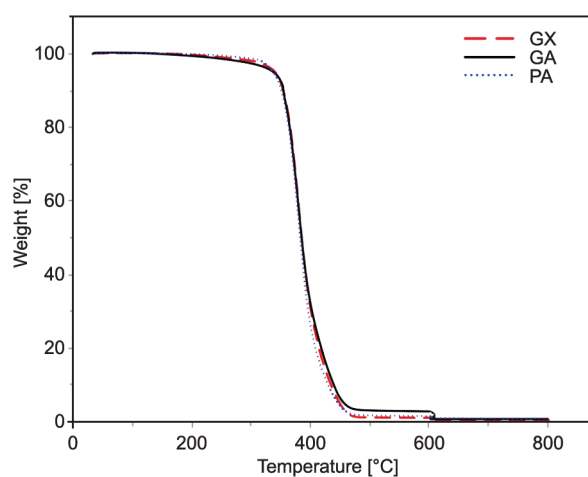


Figure 6. The TGA thermograms of cured NR with different bifunctional aldehydes.

Table 3. The thermal properties evaluated from DMA measurements and TGA thermograms of cured NR with different bifunctional aldehydes.

Samples	DMA	TGA		
	T_g [°C]	T_o [°C]	T_p [°C]	T_f [°C]
GX	-58.77	230.12	385.84	609.64
GA	-62.02	221.41	385.30	609.72
PA	-59.40	247.36	384.70	603.70

GX cured-NR exhibited higher T_g at -59.40 and -58.77 °C, respectively. This is due to the lengthiest linkage between the rubber chains in GA cured NR as shown in Figure 3, which exhibits higher mobility than the linkages in PA and GX cured ones. The higher mobility of rubber chains is comparable to the increased free volume and the T_g of GA cured-NR is found to be reduced [18]. In contrast, GX and PA cured-NR with shorter linkages between rubber chains exhibit lower mobility of rubber chains by decreasing the free volume which leads to the higher T_g . The thermal stability of various NR samples cured with different aldehydes has been evaluated using TGA. The TGA thermograms are shown in Figure 6 and also the onset temperature (T_o), temperature corresponding to the maximum rate (T_p) and termination temperature (T_f) are summarized in Table 3. It is observed that the PA cured-NR showed the highest T_o when compared to the other cured-NRs. This might be due to the stability of the aromatic ring present in PA molecule as the C=C bond has an energy 579 kJ/mol, which is higher than that of the C-C bond energy (357 kJ/mol) of GX and GA molecules [8, 19]. However, the thermal stability of cured-NRs is increased due to the formation of crosslinks by the addition of curing agents into NR as reflected in T_p and T_f values of cured-NRs.

Temperature scanning stress relaxation (TSSR)

TSSR is a technique developed by Wu *et al.* [20] to evaluate the thermal-mechanical behavior of elastomers. The cured-NR samples have been undergone characterization under isothermal and non-isothermal relaxation processes. The normalized force-temperature curves are plotted (Figure 7). In terms of T_{10} , T_{50} and T_{90} indicate the temperature at the force has been reduced by about 10, 50 and 90% from the initial force, and they are summarized in Table 4. It is observed that the PA cured NR exhibits the highest T_{10} and T_{50} at 56.8 and 94.4 °C, respectively, when compared to the cured NRs with GX and GA. A

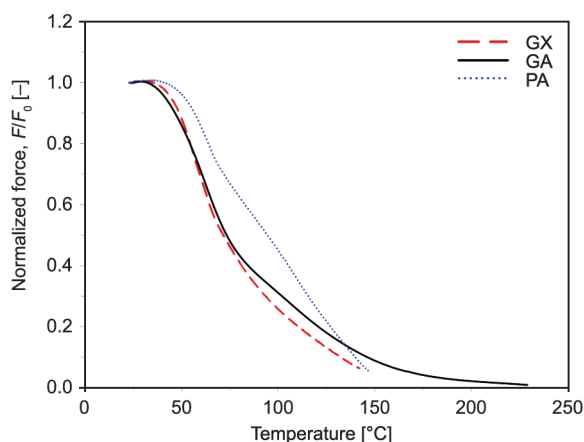


Figure 7. The normalized force as a function of temperature of cured NR with different bifunctional aldehydes.

Table 4. Degradation temperature and crosslink density obtained from the TSSR of cured NR with different bifunctional aldehyde curing agent.

Samples	σ_0 [MPa]	T_{10} [°C]	T_{50} [°C]	T_{90} [°C]
GX	0.18	49.0	71.5	131.8
GA	0.84	46.8	73.3	145.4
PA	0.22	56.8	94.4	139.5

similar trend in the thermal stability is observed in the T_{90} values of cured NR as seen in the thermograms of TGA. This is attributed to the better thermal stability of the aromatic ring in its structure. GA cured NR is thermally more stable up to 145.4 °C due to the formation of entanglements and crosslinks.

To clarify the molecular phenomenon, the relaxation spectrum $H(T)$ has been calculated by differentiating $E(T)$ with respect to temperature T using Equation (2) [20]:

$$H(T) = -T \left(\frac{dE(T)}{dT} \right)_{v = \text{const}} \quad (3)$$

The relaxation spectrum $H(T)$ as a function of temperature for different cured NRs is shown in Figure 8. It shows two significant peaks, the first peak at 50–75 °C might be assigned to the molecular chain relaxation, including de-bonding of physical interaction of NR molecules [16]. Also, it is attributed to the decomposition of branch points of the α -terminal group in NR molecules [12, 20]. The second broad peak at 90–150 °C corresponds to the chemical relaxation of cured-NRs. It is attributed to the decomposition of rubber crosslinks by aldehyde curing agents [16]. Cured-NR by GA shows a major change in the relaxation behavior when compared to other

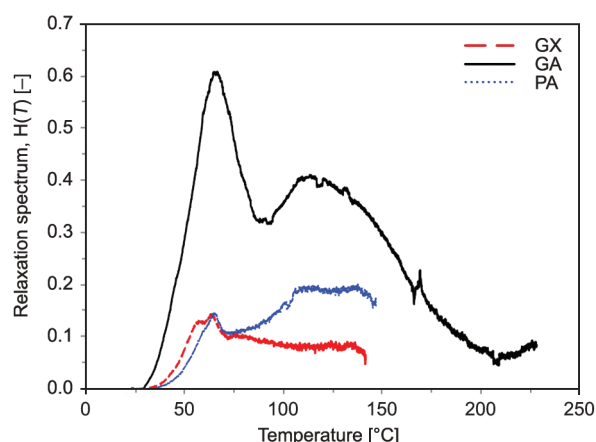


Figure 8. The relaxation spectrum as a function of temperature of cured NR with different bifunctional aldehydes.

peaks. This relaxation behavior correlates well with the crosslink density of cured-NRs. Higher crosslink density leads to elevating the relaxation of NR.

4.3 Colorimetric parameters

The perception of color is a psychophysical phenomenon that starts with a chromatic light source, capable of emitting electromagnetic radiation with wavelengths between 400–700 nm. This radiation reflects back from the surface of the object and reaches our eyes [21]. A color model (or color space) is a mathematical model to describe different colors in the form of color components represented by three axes, as shown in Figure 9 [22]. The lightness axis is represented by L^* shows the color range from white ($L = 100$) to black ($L = 0$) through gray at the center. The red-green axis is represented by a^* that shows the color range from red ($+a^*$) to green ($-a^*$). The yellow-blue axis is represented by b^* which describes the color range from yellow ($+b^*$) to blue ($-b^*$) [22–26].

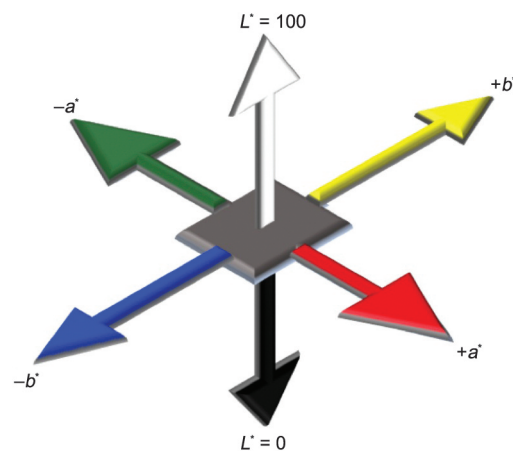


Figure 9. CIE L^* , a^* , b^* color space [22, 27].

Saturation of color depends on the amount of grey component at the center of color space and the saturation increases from the center towards a negative direction [1, 24–26].

The color analysis of NR vulcanizates can be done according to CIE (Commission Internationale de l’Eclairge), which describes different colors in the form of numbers or color components. XYZ coordinates depict the specific location of the color in the Cartesian coordinates system [27] and could be expressed in CIE L^* , a^* , b^* scale [22] as Equations (4)–(6):

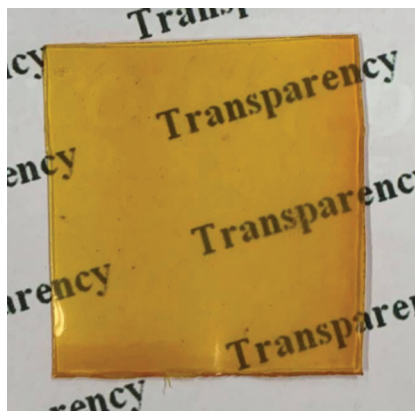
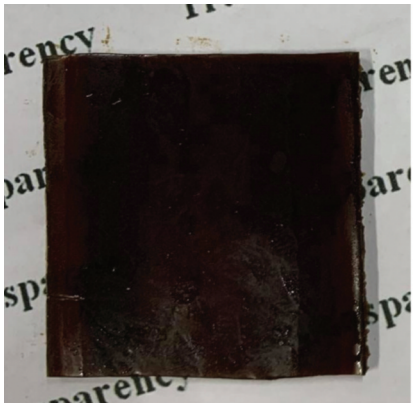

$$L^* = 116\left(\frac{Y}{Y_n}\right)^{\frac{1}{3}} - 16 \tag{4}$$

$$a^* = 500\left[\left(\frac{X}{X_n}\right)^{\frac{1}{3}} - \left(\frac{Y}{Y_n}\right)^{\frac{1}{3}}\right] \tag{5}$$

$$b^* = 200\left[\left(\frac{Y}{Y_n}\right)^{\frac{1}{3}} - \left(\frac{Z}{Z_n}\right)^{\frac{1}{3}}\right] \tag{6}$$

If $\frac{X}{X_n}, \frac{Y}{Y_n},$ and $\frac{Z}{Z_n} < 0.008856$

Table 5. The color values including L^* , a^* , b^* and physical appearance of cured NR with different bifunctional aldehydes.

Samples	L^*	a^*	b^*	Physical appearance
GX	26.86±0.05	5.81±0.12	2.98±0.08	
GA	74.28±0.08	9.88±0.11	71.52±0.24	
PA	88.16±0.23	-3.70±0.03	17.12±0.76	

where X , Y and Z are tristimulus values and X_n , Y_n and Z_n are tristimulus values for a perfect reflecting diffuser (white) [22].

Color and transparency are the apparent properties of NR films while manufacturing articles including medical devices, packaging film, and so on. The physical appearance and the color parameter of different cured-NRs are summarized in Table 5. GA and PA cured NR samples are found to be more transparent films. The PA and GA-cured NRs exhibited a higher L^* value than that of GX cured NR. It can be seen that samples with the highest brightness and saturation value appeared more transparent. On the other hand, GX cured NR is observed the lowest L^* value at 26.86 approaches to zero, indicating its black color. For a^* values of GX, GA and PA cured NR films are 5.81, 9.88 and -3.70 , respectively. All these values might not be significantly different from the red-green color. The GA cured NR exhibited the highest b^* value that related to the high yellow saturation of the NR film. The transparent films of PA and GA cured NR might be due to the chemical reaction of PA and GA with the protein present in NR latex that reduces discoloration by inhibiting the reaction between quinone and protein [6, 7]. However, the yellowish of NR films still appears due to presence of natural carotenoids in NR latex [5].

5. Conclusions

Vulcanization of NR latex using GX, GA and PA bifunctional aldehydes as the curing agents was successfully prepared at low temperature (50°C) without any specific activators and accelerators. Crosslinking of NR molecule was confirmed from the ATR-FTIR spectrum, and the crosslink density was measured using the TSSR technique. The properties in terms of mechanical, thermal and optical properties were investigated. It was observed that the GA cured NR showed superior mechanical properties such as elastic modulus, tensile strength and hardness. The thermal properties obtained from TGA and TSSR measurements, GX and PA cured NRs enhanced higher thermal stability than that of GA cured ones. Furthermore, PA cured NR exhibited superior mechanical properties (tensile strength and elongation at break), and thermal stability and showed the most transparent NR film, which expands the application of NR products such as soft robots or soft sensors and others.

Acknowledgements

This study was supported by research grants from the Royal Golden Jubilee (RGJ) Ph.D. Program (grant no. PhD/0180/2561), the National Research and Innovation Information System (NRIIS). The authors also would like to express their gratitude to the Faculty of Science, Prince of Songkla University, Hat Yai Campus. Regarding German collaborators, we gratefully acknowledge the facility support from the Faculty of Engineering and Computer Science, University of Applied Sciences Osnabrück, Germany. The authors also would like to thank King Mongkut's University of Technology Thonburi for the technical support.

References

- [1] Wichaita W., Promlok D., Sudjaiiparat N., Sripraphot S., Suteewong T., Tangboriboonrat P.: A concise review on design and control of structured natural rubber latex particles as engineering nanocomposites. *European Polymer Journal*, **159**, 110740 (2021).
<https://doi.org/10.1016/j.eurpolymj.2021.110740>
- [2] Kim C., Beuve J. S., Guilbert S., Bonfils F.: Study of chain branching in natural rubber using size-exclusion chromatography coupled with a multi-angle light scattering detector (SEC-MALS). *European Polymer Journal*, **45**, 2249–2259 (2009).
<https://doi.org/10.1016/j.eurpolymj.2009.05.015>
- [3] Luo K., You G., Zhao X., Lu L., Wang W., Wu S.: Synergistic effects of antioxidant and silica on enhancing thermo-oxidative resistance of natural rubber: Insights from experiments and molecular simulations. *Materials and Design*, **181**, 107944 (2019).
<https://doi.org/10.1016/j.matdes.2019.107944>
- [4] Rojruthai P., Kantaram T., Sakdapipanich J.: Impact of non-rubber components on the branching structure and the accelerated storage hardening in *Hevea* rubber. *Journal of Rubber Research*, **23**, 353–364 (2020).
<https://doi.org/10.1007/s42464-020-00063-7>
- [5] Sakdapipanich J., Insom K., Phupewkeaw N.: Composition of color substances of *Hevea brasiliensis* natural rubber. *Rubber Chemistry and Technology*, **80**, 212–230 (2007).
<https://doi.org/10.5254/1.3539403>
- [6] Rojruthai P., Pareseecharoen C., Sakdapipanich J.: Physical decoloration in the concentration process of natural rubber. *SPE Polymers*, **2**, 210–216 (2021).
<https://doi.org/10.1002/pls2.10049>
- [7] Lv M., Fang L., Yu H., Rojruthai P., Sakdapipanich J.: Discoloration mechanisms of natural rubber and its control. *Polymers*, **14**, 764 (2022).
<https://doi.org/10.3390/polym14040764>
- [8] Lehman N., Yung-Aoon W., Songtipya L., Johns J., Saetung N., Kalkornsurapranee E.: Influence of functional groups on properties of styrene grafted NR using glutaraldehyde as curing agent. *Journal of Vinyl and Additive Technology*, **25**, 339–346 (2019).
<https://doi.org/10.1002/vnl.21700>

- [9] Johns J., Nakason C., Thitithammawong A., Klinpituksa P.: Method to vulcanize natural rubber from medium ammonia latex by using glutaraldehyde. *Rubber Chemistry and Technology*, **85**, 565–575 (2012).
<https://doi.org/10.5254/rct.12.88920>
- [10] Hermanson G. T.: Homobifunctional crosslinkers. in ‘Bioconjugate techniques’ (ed.: Hermanson G. T.) Elsevier, Amsterdam (2013).
<https://doi.org/10.1016/B978-0-12-370501-3.00004-7>
- [11] Kalkornsurapranee E., Yung-Aoon W., Thongnuanchan B., Thitithammawong A., Nakason J., Johns J.: Influence of grafting content on the properties of cured natural rubber grafted with PMMAs using glutaraldehyde as a cross-linking agent. *Advances in Polymer Technology*, **37**, 1478–1485 (2017).
<https://doi.org/10.1002/adv.21806>
- [12] Promsung R., Nakaramontri Y., Uthaipan N., Kummerlöwe C., Johns J., Vennemann N., Kalkornsurapranee E.: Effects of protein contents in different natural rubber latex forms on the properties of natural rubber vulcanized with glutaraldehyde. *Express Polymer Letters*, **15**, 308–318 (2021).
<https://doi.org/10.3144/expresspolymlett.2021.27>
- [13] Kalkornsurapranee E., Yung-Aoon W., Songtipya L., J. Jobish.: Effect of processing parameters on the vulcanisation of natural rubber using glutaraldehyde. *Plastics, Rubber and Composites*, **46**, 258–265 (2017).
<https://doi.org/10.1080/14658011.2017.1323610>
- [14] Vennemann N., Bökamp K., Bröker D.: Crosslink density of peroxide cured TPV. *Macromolecular Symposia*, **245–246**, 641–650 (2006).
<https://doi.org/10.1002/masy.200651391>
- [15] Coates J.: Interpretation of infrared spectra, A practical approach. in ‘Encyclopedia of Analytical Chemistry: Applications, Theory and Instrumentation’ (ed.: Meyers R. A.) 1–23 (2006).
<https://doi.org/10.1002/9780470027318.a5606>
- [16] Promsung R., Nakaramontri Y., Kummerlöwe C., Johns J., Vennemann N., Saetung N., Kalkornsurapranee E.: Grafting of various acrylic monomers on to natural rubber: Effects of glutaraldehyde curing on mechanical and thermo-mechanical properties. *Materials Today Communications*, **27**, 102387 (2021).
<https://doi.org/10.1016/j.mtcomm.2021.102387>
- [17] Zhao F., Bi W., Zhao S.: Influence of crosslink density on mechanical properties of natural rubber vulcanizates. *Journal of Macromolecular Science Part B Physics*, **50**, 1460–1469 (2011).
<https://doi.org/10.1080/00222348.2010.507453>
- [18] Jiang X., Yang C. Z., Tanaka K., Takahara A., Kajiyama T.: Effect of chain end group on surface glass transition temperature of thin polymer film. *Physics Letters A*, **281**, 363–367 (2001).
[https://doi.org/10.1016/S0375-9601\(01\)00150-5](https://doi.org/10.1016/S0375-9601(01)00150-5)
- [19] Batsanov S. S., Kozhevina L. I.: Energy of the C=C double bond. *Russian Journal of General Chemistry*, **74**, 314–315 (2004).
<https://doi.org/10.1023/B:RUGC.0000025528.22795.be>
- [20] Wu M., Heinz M., Vennemann N.: Investigation of unvulcanized natural rubber by means of temperature scanning stress relaxation measurements. *Advanced Materials Research*, **718–720**, 117–123 (2013).
<https://doi.org/10.4028/www.scientific.net/AMR.718-720.117>
- [21] Plataniotis K. N., Venetsanopoulos A. N.: Color image processing and applications. Springer, Berlin (2000).
- [22] Siddiqui A., Nazzal S.: Measurement of surface color as an expedient QC method for the detection of deviations in tablet hardness. *International Journal of Pharmaceutics*, **341**, 173–180 (2007).
<https://doi.org/10.1016/j.ijpharm.2007.04.006>
- [23] Kulcu R.: Determination of the effects of different packaging methods and materials on storage time of dried apple. *MATTER: International Journal of Science and Technology*, **4**, 238–255 (2018).
<https://doi.org/10.20319/mijst.2018.42.238255>
- [24] Balaji U., Pradhan S. K.: Titanium anodisation designed for surface colouration – Systemisation of parametric interaction using response surface methodology. *Materials and Design*, **139**, 409–418 (2018).
<https://doi.org/10.1016/j.matdes.2017.11.026>
- [25] Zhang J., Koubaa A., Xing D., Liu W., Wang Q., Wang X., Wang H.: Improving lignocellulose thermal stability by chemical modification with boric acid for incorporating into polyamide. *Materials and Design*, **191**, 108589 (2020).
<https://doi.org/10.1016/j.matdes.2020.108589>
- [26] Song H. J., Kim D. H., Lee T. H., Moon D. K.: Emission color tuning of copolymers containing polyfluorene, benzothiadiazole, porphyrin derivatives. *European Polymer Journal*, **48**, 1485–1494 (2012).
<https://doi.org/10.1016/j.eurpolymj.2012.06.002>
- [27] Berberich J., Dee K-H., Hayauchi Y., Pörtner C.: A new method to determine discoloration kinetics of uncoated white tablets occurring during stability testing-an application of instrumental color measurement in the development pharmaceutics. *International Journal of Pharmaceutics*, **234**, 55–66 (2002).
[https://doi.org/10.1016/S0378-5173\(01\)00947-4](https://doi.org/10.1016/S0378-5173(01)00947-4)